USE OF GFRP RC DECKS FOR I-BEAM AND NEXT BEAM BRIDGES

Jianwei Huang, Ph.D., P.E., M.PCI, Assistant Professor, Department of Civil Engineering, Southern Illinois University Edwardsville. Edwardsville, IL
Jonathan Davis, Graduate assistant, Department of Civil Engineering, Southern Illinois University Edwardsville, Edwardsville, IL

ABSTRACT
Recently, the PCI northeast bridge technical committee developed northeast extreme tee (NEXT) beam sections that were able to serve as good substitutes for adjacent box beam bridges (w/o deck type). The NEXT type F beam bridges can offer a good long-term durability and accelerate the construction process. Despite of many advantages of the NEXT beams, in cold regions, the conventional steel reinforced concrete bridge deck is the most vulnerable component in a bridge as the deck is directly exposed to heavy de-icing salts in winter seasons. In this sense, in order to achieve a 100+ year NEXT beam bridge in cold areas, a more durable bridge deck is needed. Utilizing a GFRP RC bridge deck can be an excellent solution. In this paper, several GFRP RC decks on the NEXT beams and AASHTO I-beams were designed in accordance with the AASHTO specifications for GFRP RC bridge decks, followed by 3-D finite element simulations to examine the tensile stresses in the GFRP bars in the NEXT beam and I-beam bridges. The results from this paper showed that the AASHTO specifications are suitable for designing bridge decks in the NEXT beam bridges. Due to the 4 in. thick top flange in the NEXT beam, the bottom GFRP bars in the deck can be designed with a reduced flexure moment.

Keywords: Bridge Deck, Finite Element (FE), GFRP bar, NEXT Beam

INTRODUCTION

Nowadays, it becomes very important to develop novel bridge systems that are able to enhance the sustainability and long-term durability of highway bridges in the US. In past years, the PCI northeast bridge technical committee developed a series of northeast extreme tee (NEXT) beam sections which can offer several advantages over some of the existing types of beams (e.g. adjacent box beams)[1], including: (1) no intermediate diaphragms are needed; (2) no installation or stripping of formwork is required in the field that can accelerate the construction process[1]. According to the guidelines for Northeast Extreme Tee Beam[14], there are 8 different cross sections for the NEXT type F beams, in terms of beam depth and beam width, as shown in Figure 1[1,14].

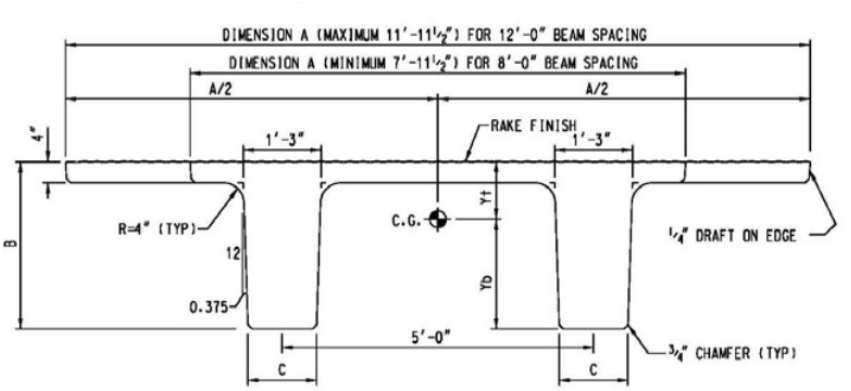

NEXT BEAM - SECTION PROPERTIES

BEAM DESIGNATION	BEAM WIDTH INCHES	BEAM DEPTH INCHES	BASE STEM WIDTH INCHES	AREA IN²	I IN⁴	Yb INCHES	Yt INCHES	St IN³	Sb IN³	WEIGHT PLF
	A	B	C			D	E			
MINIMUM WIDTH BEAMS										
NEXT 36 F	95.50	36.00	13.00	1287	160240	21.77	14.23	11261	7361	1341
NEXT 32 F	95.50	32.00	13.25	1182	115813	19.51	12.49	9272	5936	1231
NEXT 28 F	95.50	28.00	13.50	1075	79901	17.24	10.76	7426	4635	1120
NEXT 24 F	95.50	24.00	13.75	966	51823	14.95	9.05	5726	3466	1006
MAXIMUM WIDTH BEAMS										
NEXT 36 F	143.50	36.00	13.00	1479	185525	23.36	12.64	14678	7942	1541
NEXT 32 F	143.50	32.00	13.25	1374	134258	20.98	11.02	12183	6399	1431
NEXT 28 F	143.50	28.00	13.50	1267	92661	18.57	9.43	9826	4990	1320
NEXT 24 F	143.50	24.00	13.75	1158	60045	16.12	7.88	7620	3725	1206

Fig. 1 Section Properties of NEXT Beams (type F)[1,14]

As can be seen, the section depth varies from 24 in. to 36 in., whereas the beam width varies from 8 ft to 12 ft. Note that each NEXT beam consists of two stems with a spacing of 5 ft on centers. Each side of the NEXT beam has a 4 in. thick top flange, which can act as a permanent formwork for the top 8 in. thick concrete deck. The 8 in. concrete deck provides a protection for the NEXT beams from environmental attacks, especially from the deicing salts' erosion. As reported, each year large amounts of de-icing salts were used for snow/ice removal in the cold regions such as northern US and Canada[2,3], which has caused early deteriorations of various reinforced concrete (RC) bridge decks. As stated in the Federal Highway Administration (FHWA) corrosion report[2]: *"…The annual direct cost of corrosion for highway bridges is estimated to be $8.29 billion, consisting of $3.79 billion for the*

annual cost to replace structurally deficient bridges over the next ten years plus $2.00 billion for maintenance and cost of capital for concrete bridge decks plus $2.00 billion for maintenance and cost of capital for substructures and superstructures (minus decks) plus $0.50 billion for the maintenance painting cost for steel bridges." It should be also noted that indirect costs due to traffic delays and lost productivity were estimated to be more than 10 times the direct cost[2]. In order to combat the corrosion and improve the sustainability of bridge deck structures, significant efforts have been made in the past years by exploring the use of special reinforcements, such as galvanized steel reinforcements and epoxy coated steel reinforcements[3]. However, feedbacks from the field showed that such solutions cannot eliminate the steel corrosion in the bridge decks[3,4]. In this regard, in order to achieve a bridge with a 100+ year service life span, novel types of bridge decks shall be considered. In recent years, fiber reinforced polymer (FRP) reinforcements have been considered as promising substitutes to the conventional steel reinforcements since the FRPs are non-metallic[3]. In the concrete industry, Glass-FRP (GFRP) bars are preferred since they have lower costs than Carbon-FRPs (CFRPs). To date, several design guidelines have been developed for the use of FRP bars in concrete structures/bridges, including, (1)ACI 440.1R-06 (2006)[3]; (2) AASHTO LRFD Bridge Design Guide Specifications for GFRP-Reinforced Concrete Bridge Decks and Traffic Railings (2009)[5]; (3) CHBDC (2006), Canadian Standards Association International[6]; (4) CSA-S806 (2002), Canadian Standards Association[7]. In order to validate the existing design guides, a number of GFRP RC bridge decks have been constructed in the US and Canada[8,9,10], many of which were instrumented and tested by moving vehicles[9,10]. Regarding the FRP technology, one of the concerns is the long-term durability of GFRP materials in the concrete[3,8,13]. This concern was raised from various durability tests in the lab[3,11,12,13]. As reported, the GFRP bars experienced a reduction in tensile strength when the bars were subjected to environmental exposures combined with sustained loadings[11,12]. In the current GFRP RC design guides, a stress limit not exceeding 20% of the GFRP design strength is required for a design at service limit states[3,5]. Huang (2014)[13] assessed the creep requirements for stress levels in the GFRP bars in RC bridge decks by a comprehensive parametric study per AASHTO LFRD GFRP design guide specifications, which revealed that the stress levels in the GFRP bars in real bridge decks are much lower than the guide-required limit[13]. With this being said, the GFRP bars shall have an excellent durability in the concrete decks. In light of the above discussions, utilizing GFRP RC bridge decks in the NEXT beam bridges can provide an excellent durability, thus offering a viable solution to achieve 100+ year bridges in the US.

The 1st edition of the guidelines for the Northeast Extreme Tee Beam (NEXT beam) was published in 2012[14], whereas the current AASHTO design specifications for GFRP bridge decks was released in 2009[5], which implied the NEXT beam sections were not considered in the current AASHTO GFRP specifications[5]. Thus, it is necessary to examine the suitability of the current AASHTO specifications[5] for designing a GFRP deck on the NEXT beams. Unlike I-shaped beams, the NEXT beams have a 4 in. thick flange, which may act as a part of the top deck and participate in carrying deck loads. In this paper, the tensile strains in the GFRP bars in the NEXT beam bridge decks were compared to that in the I-beam bridge decks, through using 3-D finite element (FE) simulations.

VALIDATION OF 3-D FINITE ELEMENT MODELING IN ABAQUS

In order to assure the accuracy of FE simulations as proposed in this paper, a field-tested bridge was adopted for verification. Abaqus[15], a popular FE program, was employed for the numerical simulations. EI-Salakawy et al. (2005)[10] conducted a field load test on a GFRP RC bridge deck as located in Canada. In this bridge[10]: it was simply-supported and had a span length of 85.4 ft (26.04 m); it consisted of five AASHTO Type IV girders spaced at 8.86 ft (2.7 m) on centers, with an overhang of 4.6 ft (1.40 m) on each side; the deck had a thickness of 8 in. (200 mm), and a concrete strength of 5 ksi (35 MPa); No.6 GFRP bars were used with a spacing of 3 in. (75 mm) and 4 in. (100 mm) for the top and bottom transverse bars, respectively; the GFRP bars had an E-modulus of 6091.6 ksi (42 GPa) and a guaranteed tensile strength of 78 ksi (540 MPa)[10]. After the bridge was constructed, a field load test was conducted to measure the tensile strains in the GFRP reinforcements[10]. As reported, for the single truck for Path D, the maximum measured strain at Gauge B2 in the bottom transverse GFRP bar was 30 με[10].

The above tested bridge was modeled in Abaqus with solid elements for the concrete deck and girders, whereas bar elements were used for the GFRP reinforcements. The test truck was mimicked as point loads placed at the specified location (single truck, Path D) as indicated in EI-Salakawy et al. (2005)[10]. Linear material properties were used for both GFRP bars and concrete since the loadings in the load test was under service limit states. The FE simulation gave a tensile strain of 33 με at B2 gage location, as shown in Figure 2, which indicated the FE result has an excellent agreement with the reported strain[10] (i.e., 30 με). As can be seen, the FE modeling can accurately capture the structural response of the GFRP RC decks under external loads. With confidence, Abaqus was employed in this paper to simulate the NEXT beam bridges and I-shaped beam bridges, as discussed in the following sections.

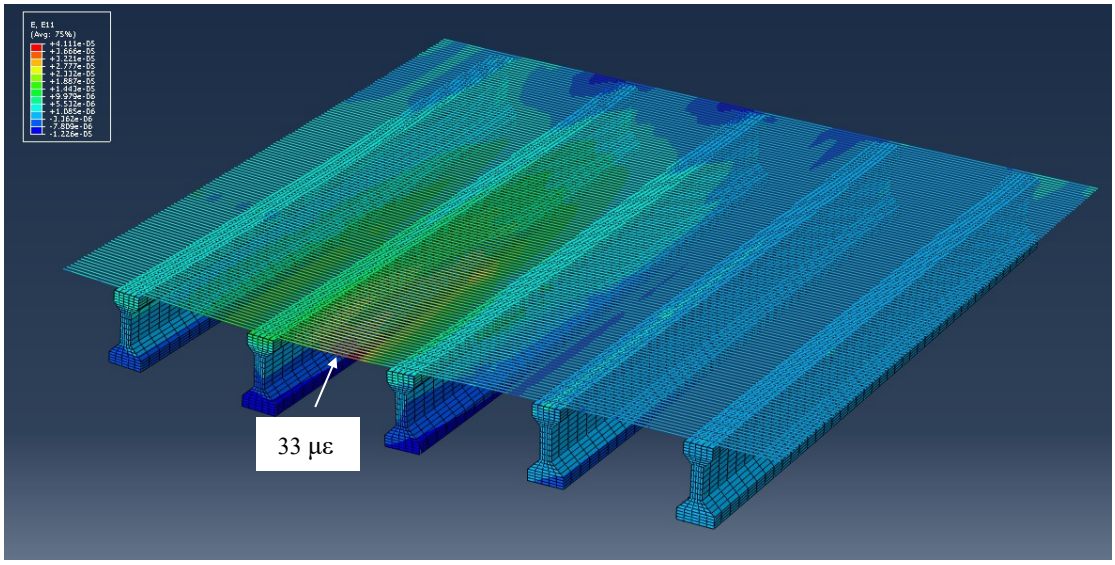

Fig. 2 Strain contour in the bottom GFRP bars under the test truck

DESIGN OF GFRP BAR REINFORCED CONCRETE DECK PER AASHTO DESIGN GUIDE SPECIFICATIONS FOR GFRP RC BRIDGE DECKS[5]

The following summarizes the deck design methodology in the AASHTO GFRP design specifications[5]. Unlike steel reinforced concrete, both over-reinforced section ($\rho_f > \rho_{fb}$) and under-reinforced section ($\rho_f < \rho_{fb}$) are allowed for the GFRP reinforced concrete[3,5], where ρ_f is the reinforcing ratio and ρ_{fb} is the balanced reinforcing ratio, which can be calculated as below:

$$\rho_f = \frac{A_f}{b \cdot d} \qquad \text{(Ref. [5])}$$

$$\rho_{fb} = 0.85 \cdot \beta_1 \cdot \frac{f_c'}{f_{fd}} \cdot \frac{E_f \cdot \varepsilon_{cu}}{E_f \cdot \varepsilon_{cu} + f_{fd}} \qquad \text{(AASHTO 2.7.4.2-2[5])}$$

Where f_{fd} is the GFRP design strength, which is defined as below:

$$f_{fd} = C_E \cdot f_{fu} \qquad \text{(AASHTO 2.6.1.2-1[5])}$$

Where C_E is the environmental reduction factor (C_E=0.8 and C_E=0.7 for concrete elements non-exposed and exposed to the earth and weather, respectively[5]).

For a flexural design, when $\rho_f < \rho_{fb}$, the nominal flexural strength M_n is calculated with AASHTO Eq. 2.9.3.2.2-3, while AASHTO Eq. 2.9.3.2.2-1 is used to compute M_n when $\rho_f > \rho_{fb}$.

$$M_n = A_f f_{fd} (d - \frac{\beta_1 c_b}{2}) \qquad \text{(AASHTO 2.9.3.2.2-3[5])}$$

$$c_b = (\frac{\varepsilon_{cu}}{\varepsilon_{cu} + \varepsilon_{fd}}) \cdot d \qquad \text{(AASHTO 2.9.3.2.2-4[5])}$$

$$M_n = A_f f_f (d - \frac{a}{2}) \qquad \text{(AASHTO 2.9.3.2.2-1[5])}$$

Where "a" is the depth of equivalent rectangular stress block; f_f is the effective tensile strength in GFRP bar, as follows:

$$f_f = (\sqrt{\frac{(E_f \varepsilon_{cu})^2}{4} + \frac{0.85 \beta_1 f_c'}{\rho_f} E_f \varepsilon_{cu}} - 0.5 E_f \varepsilon_{cu}) \leq f_{fd} \qquad \text{(AASHTO 2.9.3.1-1[5])}$$

In the LRFD design method, resistance factors, ϕ, shall be applied to the nominal flexural resistance to account for structural ductility, as follows:

$$M_r = \phi \cdot M_n \qquad \text{(AASHTO 2.9.3.2.1-1[5])}$$

In order to avoid the creep rupture of a GFRP bar under sustained loadings, or failure due to fatigue loading, the stress levels, f_{fs}, in the GFRP bars are limited not exceeding 20% of the GFRP design strength[5]. In addition, the minimum flexural tensile reinforcement requirement shall be checked, as follows:

$$A_{f,\min} \geq \max(0.16\sqrt{f_c'};0.33)\frac{bd}{f_{fd}} \qquad \text{(AASHTO 2.9.3.3-1[5])}$$

Furthmore, the maximum crack width shall be limited within 0.02 in, as follows:

$$w = 2\frac{f_{fs}}{E_f}\beta k_b\sqrt{d_c^2 + \frac{s^2}{4}} \leqq 0.02 \text{ in.} \qquad \text{(AASHTO 2.9.3.4-1[5])}$$

Table 1 showed the AASHTO LRFD load combinations[16] for each requirement in the AASHTO GFRP design specifications[5].

Table 1 Load combinations for different limit states

Limit states	AASHTO Requirements[5]	LRFD load combinations[16]
Flexural resistance	$M_u < \phi M_n$	Strength I
Creep rupture	$f_{fs}<0.2f_{fd}$	Service I
Fatigue rupture	$f_{fs}<0.2f_{fd}$	Fatigue II
Maximum crack width requirements	w < 0.02 in.	Service I

DESIGN PARAMETERS

Dead loads: dead loads (DL) for a GFRP bridge deck shall include the deck itself, future wearing surface, and barriers[5,16]. The following unit weights were assumed and used in this study, as shown in Table 2.

Table 2 Unit weights for the deck dead loads[5,16,17]

	Concrete for deck	Barrier/each	future wearing surface
Unit weight	0.150 kcf	450 plf	25 psf

The positive and negative flexural moments due to the dead loads on a deck can be determined by using $M=wL^2/10$, as indicated in Wassef et al. (2012)[17].

Live loads: in this paper, the AASHTO LRFD Specification Table A4-1[16] was used to determine the live load (LL) effects on a bridge deck. Since the NEXT beam bridges have uneven stem spacing[1,14], the larger one was used to produce the positive and negative LL moments. More specifically, a girder spacing of 5 ft is used for the 8 ft wide NEXT beam bridges, whereas a spacing of 7 ft is used for the 12 ft wide NEXT beam bridges.

Material Properties: Normal weight concrete with 4 ksi compressive strength was used in this study. The material properties of the GFRP bars as used in this study were shown in Table 3.

Table 3 GFRP bar materials properties[3,9,18]

GFRP bar size	d_b (in.)	A_f (in.^{2})	f_{fu} (ksi)	E_f (ksi)
#5	0.625	0.31	95	5801.5
#6	0.750	0.44	90	5801.5

Concrete Cover

In this study, concrete covers (center of GFRP bar to concrete surface) of 2.0 in. and 1 in. were used for top and bottom GFRP bars, respectively.

Two NEXT beam bridges (named as Bridge I & II) were considered in this paper, one was constructed with 8 ft wide beams, whereas the other was with 12 ft wide beams. Figure 3 showed the bridge cross sections. For comparisons, this paper also investigated another two bridges with AASHTO type III beams (named as Bridge III & IV), as shown in Figure 3 as well.

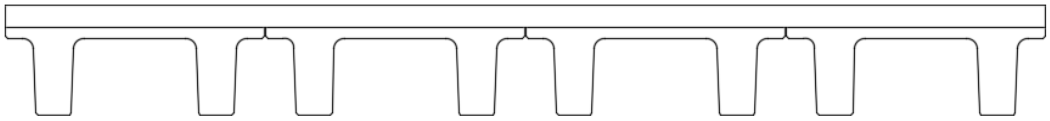

(a) Bridge I (four 8 ft wide NEXT beams)

(b) Bridge II (three 12 ft wide NEXT beams)

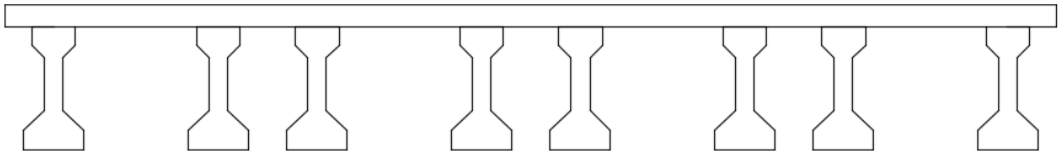

(c) Bridge III (AASHTO Type III beams, same spacing as Bridge I)

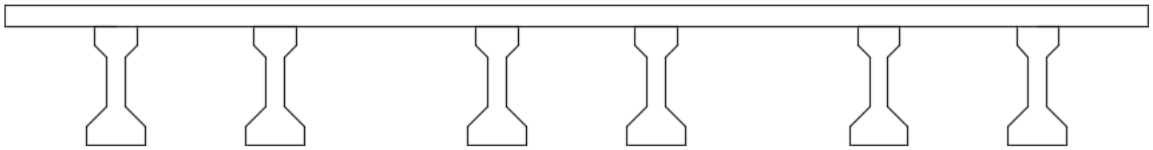

(d) Bridge IV (AASHTO Type III beams, same spacing as Bridge II)

Fig. 3 Cross sections of NEXT beam[1,14] and AASHTO I-beam[19] bridges

Note that Bridge III had the same girder spacings as Bridge I, whereas Bridge II and IV had the same girder spacings. For the above four bridges, the top and bottom GFRP bars in each bridge deck were designed in accordance with the design requirements in the AASHTO GFRP design specifications[5] and in the AASHTO LRFD bridge design specifications[16]. Note that an 8 in. thick deck was used for deck design for each of the four bridges above. Table 4 summarized the GFRP reinforcing details.

Table 4 GFRP reinforcing details

Bridge I & Bridge III	Bridge II & Bridge IV
Top GFRP bars: #5 @ 4 in.	Top GFRP bars: #6 @ 4 in.
Bottom GFRP bars: #5 @ 4.5 in.	Bottom GFRP bars: #5 @ 4 in.

FINITE ELEMENT SIMULATIONS

In Abaqus, the above four bridges were constructed in the same way as the aforementioned verified bridge. The AASHTO design loading[16] (i.e. HL-93) was used to quantify and compare the tensile strains in top and bottom GFRP bars in the four bridges. Note that the HL-93 loading consists of a design truck (i.e., HS-20) and a 0.64 k/ft design lane load (10 ft wide)[16]. In the FE simulations, the AASHTO design truck (including a 33% dynamic impact[16]) was mimicked as a set of point loads, with the middle axle being placed at the mid-span of the bridge. The design lane load was simulated as a pressure load over the design lane.

In accordance with the AASHTO LRFD specifications[16], one lane loaded and two and more lanes loaded cases shall be examined, if the bridge width permits[16]. Considering the bridge widths of the above four bridges, only one-lane and two-lane loaded cases were explored in this paper, as discussed below.

One Lane Loaded Cases

Figure 4 showed the loading profile that had only one design lane loaded, which was placed right next to the left curb[3] (named as case 1-1). In order to explore the maximum strains in GFRP bars in the deck, a number of load cases were explored by moving the load case 1-1 transversely in 1 ft increments towards the right curb direction. Due to the symmetry of the

bridge, the load case was terminated once it reached the centerline of the bridge cross section. By doing so, the maximum tensile strains in the top and bottom GFRP bars in the bridge deck were obtained for the one-lane loaded cases.

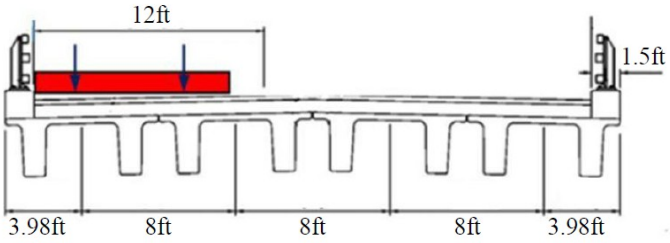

Fig. 4 Loading profile for one lane
(note: bridge section adapted from [1,14])

Two Lane Loaded Cases

Per AASHTO LRFD design specifications[16], the design lane load can appear anywhere within the traffic lane[16]. In this sense, in order to find out the most critical tensile strain in the GFRP bars, two different load profiles were investigated for the two lane loaded cases, as shown in Figures 5 and 6.

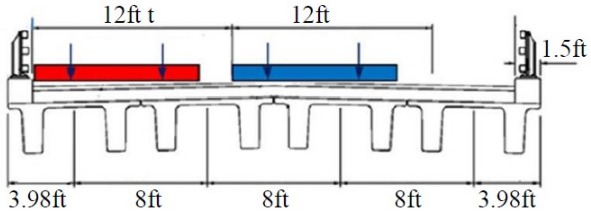

Fig 5 Loading profile #1 (2 lane)
(note: bridge section adapted from [1,14])

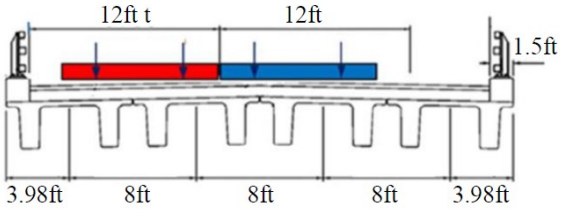

Fig. 6 Loading profile #2 (2 lane)
(note: bridge section adapted from [1,14])

Similar to the one lane loaded cases, the two adjacent lanes were initially placed next to the left curb, after which additional cases were explored by transversely moving the two loaded lanes to the right in 1 ft increments. Once the center of the two lanes reached the centerline of the bridge cross section, we stopped the exploration due to the symmetry of the bridge.

For the Bridge I and Bridge III, a total of 10 cases and 9 cases were explored for the one-lane and two-lane loaded cases, respectively. Whereas, for the Bridge II and Bridge IV, a total of 12 and 11 cases were examined for the one-lane and two-lane loaded cases, respectively. After running the analysis of each case, the maximum tensile strains in the top and bottom GFRP bars were obtained and compiled for further study, as discussed below.

RESULTS AND DISCUSSIONS

The FE results of the tensile strains in the top GFRP bars were compiled and plotted in Figures 7 and 8. In the horizontal axis in Figure 7, cases No.1 to No.10 were one-lane loaded cases, whereas cases No.11 to No.19 were two lane loaded cases. In Figure 8, cases No.1 to No.12 were one-lane loaded cases, whereas cases No.13 to No.23 were two lane loaded cases.

As can be seen from Figure 7, the maximum tensile strains in the top GFRP bars were very close between the NEXT beam and I-beam bridges for all of the cases being explored. Since the same GFRP reinforcements were used in Bridge I (NEXT beam) and Bridge III (I-beam), it implied that the 4 in. thick flange in the 8 ft wide NEXT beams had negligible influence on the stresses in the top GFRP bars. From Figure 8, the same observations can be made for the 12 ft wide NEXT beam bridge. These were interesting observations, which can be said that the current AASHTO design specifications[5,16] can be directly applied to the design of NEXT beam bridge decks at negative moment regions with using the actual deck thickness in the deck design. In addition, it can be noticed that the maximum tensile strains in the top bars in all the four bridges were less than 120 με (equal to a tensile stress of 0.70 ksi), which accounted for less than 1% of the GFRP tensile strength.

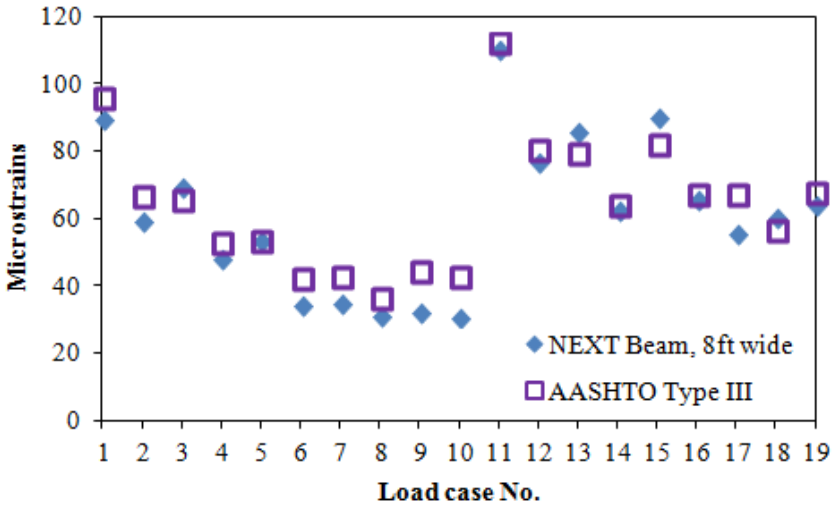

Fig. 7 Max. tensile strains in the top GFRP bars (Bridges I & III)

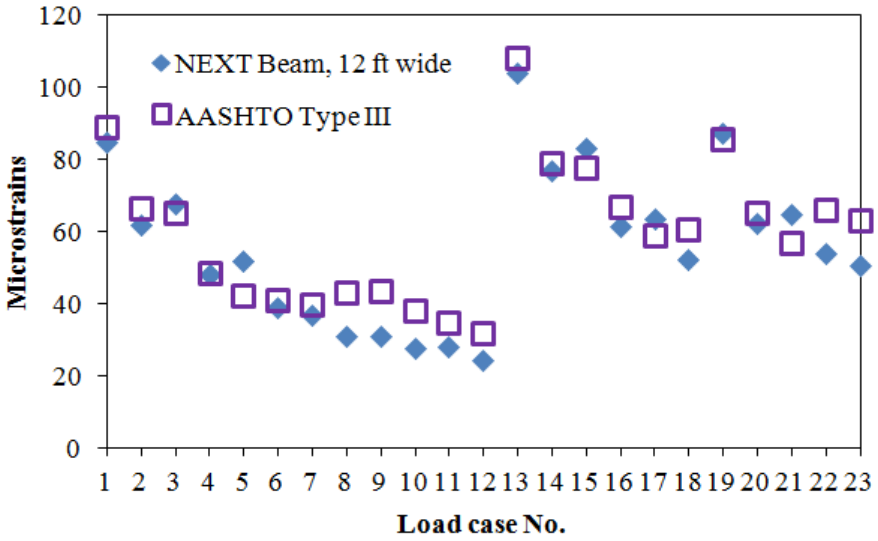

Fig. 8 Max. tensile strains in the top GFRP bars (Bridges II & IV)

Figures 9 and 10 showed the FE results of the tensile strains in the bottom GFRP bars in the bridge decks. In the horizontal axis in Figure 9, cases No.1 to No.10 were one-lane loaded cases, whereas cases No.11 to No.19 were two lane loaded cases. In Figure 10, cases No.1 to No.12 were one-lane loaded cases, whereas cases No.13 to No.23 were two lane loaded cases. In each figure, the tensile strains in the bottom GFRP bars were compared between the NEXT beam and I-shaped beam bridges. As can be seen from Figure 9, the maximum tensile strain in the bottom GFRP bars in Bridge III (I-beam) were higher than that in Bridge I (NEXT beam), which indicated that the 4 in. top flange in the NEXT beam actually contributed in carrying the positive moments in the deck. The same observations can be found in Figure 10 that the maximum strains in the bottom bars in the NEXT beam bridge are less than that in the I-beam bridge, which reassure the contribution of the NEXT beam top flange in carrying the deck positive moments.

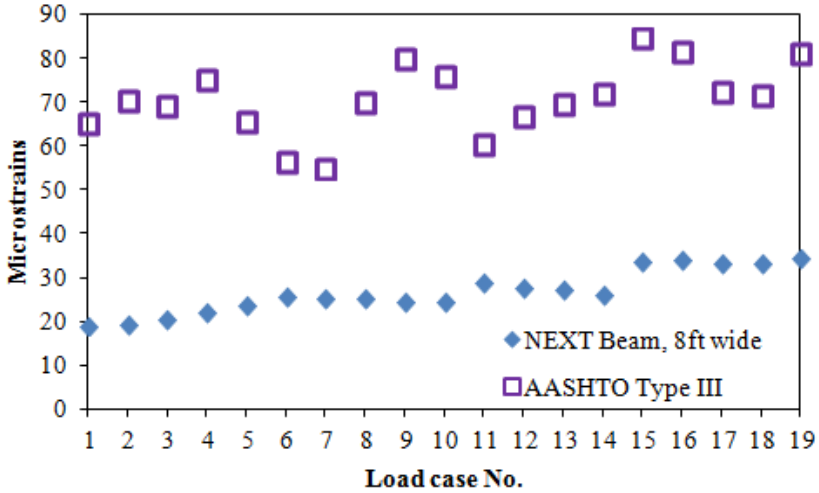

Fig. 9 Max. tensile strains in the bottom GFRP bars (Bridges I & III)

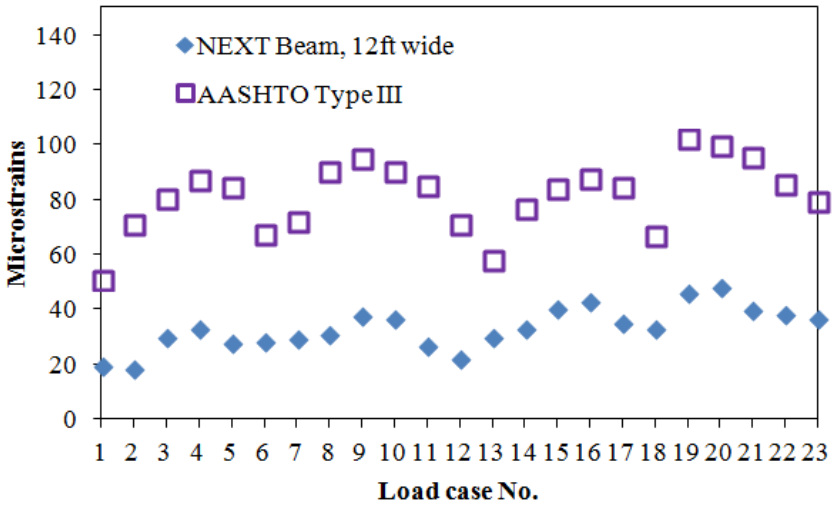

Fig. 10 Max. tensile strains in the bottom GFRP bars (Bridges II & IV)

It should be noted that the maximum tensile strains in the bottom bars in all the four bridges were less than 120 με (equal to a tensile stress of 0.70 ksi), which accounts for less than 1% of the GFRP tensile strength. Thus, it can be said that the current AASHTO design specification[5,16] is also suitable for the design of the bottom GFRP bars in the NEXT beam bridge decks.

CONCLUSIONS

In this paper, several GFRP RC decks on the NEXT beams and AASHTO I-beams were designed in accordance with the AASHTO specifications[5,16]. The maximum tensile strains in the top and bottom GFRP bars in the bridge decks were examined by using 3-D finite element simulations. By comparing the tensile strains in the GFRP bars in the NEXT beam and I-beam bridge decks, the following conclusions can be made.

- The current AASHTO GFRP design specifications[5] are suitable for designing a GFRP deck in a NEXT beam bridge.
- The AASHTO GFRP design specifications[5] can be directly applied to the design of NEXT beam decks at negative moment regions. The 4 in. top flange in the NEXT beam has negligible influence on the tensile strains in the top GFRP bars.
- In positive moment regions in a NEXT beam bridge deck, the AASHTO GFRP design specifications[5] are applicable as well. If compared to a deck on an I-beam bridge, the design positive moment in a NEXT beam bridge deck can be slightly reduced, but further research is required for such reduction. Analytical and numerical study on this subject is under investigation by the authors.

Based on the findings as obtained in this paper, utilizing a GFRP RC bridge deck in a NEXT beam bridge could provide a viable solution to achieve a 100+ year bridge, even in the cold regions.

REFERENCES

1. Culmo, M.P., and Seraderian, R.L. (2010), Development of the northeast extreme tee (NEXT) beam for accelerated bridge construction, PCI Journal 55(3), 86-101.
2. Koch, G.H. et al. (2002), Corrosion costs and prevention strategies in the United States, Report No. FHWA-RD-01-156, Federal Highway Administration, Washington, D.C., USA.
3. ACI 440.1R-06, Guide for the design and construction of concrete reinforced with FRP bars, American Concrete Institute, Committee 440, Farmington Hills, MI, USA.
4. Clear, K.C., et al. (1995), Performance of epoxy-coated reinforcing steel in highway bridges, NCHRP Report 370, Transportation Research Board, Washington, D.C., USA.
5. AASHTO LRFD bridge design guide specifications for GFRP-reinforced concrete bridge decks and traffic railings (2009), AASHTO, Washington, D.C., USA.
6. CHBDC (2006), Canadian Highway Bridge Design Code, Canadian Standards Association International, Toronto, Ont., Canada.
7. CSA-S806 (2002), Design and construction of building components with fibre-reinforced polymers, Canadian Standards Association, Ont., CA.
8. Mufti, A. et al. (2011), Durability of GFRP rods in field demonstration projects across Canada, CDCC 2011 Fourth International Conference on Durability & Sustainability of FRP Composites for Construction and Rehabilitation, July 20–22, 2011, Quebec City, Quebec, Canada.
9. Benmokrane, B., El-Salakawy, E., El-Ragaby, A., & Lackey, T. (2006), Designing and testing of concrete bridge decks reinforced with glass FRP bars, Journal of Bridge Engineering, 11(2), 217-229.
10. El-Salakawy, E., Benmokrane, B., El-Ragaby, A., and Nadeau, D., Field investigation on the first bridge deck slab reinforced with glass FRP bars constructed in Canada, Journal of composites for construction, no. 6 (2005): 470-479.
11. Mukherjee, A., and Arwikar, S.J., Performance of glass fiber-reinforced polymer reinforcing bars in tropical environments - Part I: structural scale tests, ACI Structural Journal, Vol. 102, No.5 (2005): 745-753.
12. Almusallam, T.H. and Al-Salloum, Y.A., Durability of GFRP rebars in concrete beams under sustained loads at severe environments, J. of Composites for Construction, ASCE, Vol. 40, No. 7 (2006): 623-637.
13. Huang, J., GFRP Bar reinforced concrete bridge deck: assessment of the AASHTO design guide specifications, proceedings of 2014 PCI Annual Convention an Exhibition and National Bridge Conference, Sept. 6-9, 2014. Washington, DC, USA (CD-ROM).
14. Guidelines for Northeast Extreme Tee Beam (NEXT beam), First Edition, PCI Northeast, 2012, pp64.
15. Abaqus/CAE user's manual, Simulia Corp., Providence, RI, USA, 2011.
16. AASHTO LRFD bridge design specifications, 7th Edition, the American Association of State Highway and Transportation Officials, Washington, D.C., USA, 2014.
17. Wassef, W.G., Smith, C., Clancy, C.M., Smith, M.J. (2012), Comprehensive design example for prestressed concrete (PSC) girder superstructure bridge with commentary, Report #: FHWA NHI - 04-043.

18. ACI 440.6-08, Specification for carbon and glass fiber-reinforced polymer bar materials for concrete reinforcement, American Concrete Institute, Committee 440, Farmington Hills, MI, USA.
19. PCI bridge design manual, 3rd Edition, the Precast/Prestressed Concrete Institute, Chicago, IL, USA, 2011.